Moisture Absorption by Various Polyamides and Their Associated Dimensional Changes

L. Monson, M. Braunwarth, C. W. Extrand

Entegris, Inc., 3500 Lyman Boulevard, Chaska, Minnesota 55318

Received 16 February 2007; accepted 23 May 2007
DOI 10.1002/app.27057
Published online 19 September 2007 in Wiley InterScience (www.interscience.wiley.com).

ABSTRACT: The dimensional changes associated with moisture absorption were examined for various polyamides (PAs). Plaques of varying thickness were compression-molded or injection-molded and then immersed in water. Periodically, the plaques were removed from water and their mass and dimensions were measured. This was continued until they were completely saturated. The more polar PA46 absorbed more water than less polar PA6 and PA66 and therefore, was more susceptible to moisture-induced dimensional growth. For a given polymer, it was found that the thicker samples took longer to reach saturation, but had the same diffusion coefficient as thinner ones. Changes in dimensions coincided with changes in mass. Sorption and swelling followed slightly different paths, but arrived at their respective equilibrium values at the same time. Within experimental error, dimensional expansion due to water absorption was the same in all directions. Injection-molded samples absorbed slightly more water than compression-molded ones, but their absorption rates were equal. Equilibrium water absorption data were used to approximate the dimensional changes associated with the swelling of the PAs. © 2007 Wiley Periodicals, Inc. J Appl Polym Sci 107: 355–363, 2008

Key words: diffusion; polyamides; nylon; swelling; water

INTRODUCTION

Automated processes used in microelectronic fabrication facilities require plastic parts with tight, reproducible dimensional tolerances. These plastic parts often are manufactured from engineering polymers, such as polycarbonate, polysulfones, polyimides, and polyaryletherketones. These polymers are hygroscopic and absorb modest amounts of water. Moisture absorption can lead to small but significant dimensional changes, expanding parts beyond their dimensional specifications, causing disruptions in processes or destroying product. Direct measurement of these small dimensional changes often is tedious.

Our goal was to develop a simple approach to indirectly estimate the dimensional changes of thermoplastic parts from their mass uptake. Thus, a study was undertaken to understand the relation between moisture absorption and the associated dimensional changes in plastic parts using water and various PAs as a model system. Dimensional changes due to water absorption are much greater for highly hygroscopic thermoplastics, such polyamides (PAs), and consequently easier to measure. Even though the large degree of sorption and swelling associated with PAs are undesirable for most microelectronics applications, these materials are well suited for understanding how moisture absorption influences the dimensions of thermoplastic materials.

A few investigators have previously examined the dimensional changes or swelling that accompany sorption of vapor or liquid.[1–6] One of the first swelling studies of a thermoplastic polymer was performed by Crank.[1] He modeled the swelling behavior of polystyrene that had been exposed to methylene chloride. Subsequent studies generally employed small fibers[2,4] or thin films[3,5] of PA6 or PA66. In our study, we used much thicker specimens that are more representative of injection-molded plastic parts. We also employed a broader range of PAs, PA6, PA66 and PA 46.

ANALYSIS

Amide fraction

PAs, more commonly referred to as nylons, are polymers composed of methylene and amide groups. Amide fraction (x_a) was determined from number of amide groups (N_a) and the number of methylene groups (N_m) in each molecular repeat unit,

$$x_a = N_a/(N_a + N_m). \quad (1)$$

Crystallinity

The crystalline fraction (x_c) of each polymer was calculated from the measured melting enthalpy (ΔH) as

Correspondence to: C. W. Extrand (chuck_extrand@entegris.com).

Journal of Applied Polymer Science, Vol. 107, 355–363 (2008)

TABLE I
Amide Fraction, Mold Temperatures and Density of PA Pellets and Compression-Molded Plaques

			ρ_o (g/cm^3)			ρ_f (g/cm^3)	ρ_o/ρ_f
Polymer	x_a	T_{mold} (°C)	Literature	Pellet	Plaque	Plaque	Plaque
PA66	0.167	240	1.14	1.14 ± 0.01	1.15 ± 0.00	1.15 ± 0.00	0.997 ± 0.002
PA6	0.167	270	1.13	1.15 ± 0.01	1.14 ± 0.01	1.15 ± 0.01	0.993 ± 0.011
PA46	0.200	310	1.18	1.18 ± 0.00	1.18 ± 0.00	1.18 ± 0.00	0.996 ± 0.004

$$x_c = \Delta H/\Delta H_c, \tag{2}$$

where (ΔH_c) is the melting enthalpy of the 100% crystalline polymer.[7,8]

Absorption

During the early stages of sorption, the mass (m) of liquid absorbed by a thin sheet increases with time (t) as[9]

$$(\pi/16)B_o^2[(m - m_o)/(m_f - m_o)]^2 = D_t \tag{3}$$

where m_o is the initial mass, m_f is the final mass, B_o is the initial sample thickness, and D is the diffusion coefficient. The mass (m) of liquid absorbed at any time (t) is given by

$$m/m_o = 1 + S[(m_f/m_o) - 1], \tag{4}$$

where S is the following series,

$$S = 1 - \sum_{n=0}^{\infty}\{8/\pi^2(2n+1)^2 \exp[-D(2n+1)^2\pi^2 t/B_o^2]\} \tag{5}$$

Similar equations can be used to approximate dimensional changes. The change in the length (L) associated with absorption is given by

$$L/L_o = 1 + S[(L_f/L_o) - 1], \tag{6}$$

where L_o and L_f are the initial and equilibrium lengths.

The equilibrium length ratio (L_f/L_o) can be estimated from equilibrium mass absorption (m_f/m_o) as

$$L_f/L_o = [(\rho_o/\rho_f)(m_f/m_o)]^{1/3}, \tag{7}$$

where ρ_o and ρ_f are the initial and equilibrium density. If the density (ρ) of the material does not change appreciably during absorption ($\rho_o \approx \rho_f$), then eq. (7) reduces to

$$L_f/L_o = (m_f/m_o)^{1/3}. \tag{8}$$

Derivation of eqs. (6)–(8) can be found in the Appendix. Equilibrium absorption times (t_f) for a sample with an initial thickness of B_o can be estimated from the Neumann number (α),[10]

$$\alpha = t_f/B_o^2. \tag{9}$$

EXPERIMENTAL

Materials

The following homopolymers were used to mold plaques: polyamide 6 (PA6, DSM Akulon F223D), polyamide 66 (PA66, DSM Akulon S223D), and polyamide 46 (PA46, DSM Stanyl TW341). Values of initial (or dry) density (ρ_o), amide fractions (x_a), and molding temperatures (T_{mold}) are listed in Table I.[11,12] Methanol (MeOH, Fisher, Optima Grade, ρ_{MeOH} = 0.7914 g/cm^3)[13] was used for density determinations. Absorption measurements were made with 18 MΩ deionized (DI) water.

Sample preparation

Using densities (ρ_o) listed in Table I, the approximate mass of pellets ($m_{pellets}$) required for molding was determined for each resin based on the volume of the mold (V_{mold}),

$$m_{pellets} = \rho_o V_{mold}. \tag{10}$$

Since PAs tend to slowly absorb moisture from the atmosphere,[10] the drying procedure was necessary to remove any moisture that had accumulated during manufacture or storage. Each compression-molded sample was prepared using a premassed sample of pellets that had been dried in a vacuum oven at 80°C for 4 h. Upon removal from the vacuum oven, all pellets were then stored either under vacuum or in a desiccator.

Moisture content was checked with a moisture analyzer (Arizona Instruments, Computrac 2000, Phoenix, AZ) by measuring the mass loss after 10 min at 150°C. After drying, moisture content of the PA pellets was <0.2%. An electrically heated platen press was used to compression mold plaques. Molding temperatures (T_{mold}) for the compression-molded specimens are listed in Table I. PA pellets were poured into a rectangular mold and then ''sandwiched'' between two stainless steel plates lined with aluminum sheets. This sandwich was placed in the heated press with the platens closed to the first

point of contact for 2 min. After 2 min, pressure was gradually applied until 400 kg was reached. After allowing the sample to heat for another minute, the pressure was increased to 1000 kg for an additional 2 min. This assembly was removed from the press and then placed between two large aluminum plates to facilitate uniform cooling on both sides. After cooling, the plaque was removed from the steel plates and aluminum liners. The compression-molded plaques had a length (L_o) of $\sim$ 10 cm, a width (W_o) of 5 cm, and three different thicknesses (B_o): 0.8 mm, 1.6 mm, and 3.2 mm.

The injection-molded plaques were supplied by DSM Engineering Plastics. The approximate dimensions of the injection-molded samples were as follows: L_o = 12 cm, W_o = 1 cm, and B_o = 1.6 mm or B_o = 3.2 mm. These samples were also vacuum dried for 4 h at 80°C.

All samples were trimmed to remove any excess flash or surface irregularities. Each sample was scored with an identification number. Measurement marks were etched along the length and width dimensions to provide a location guide for more uniform measurements. All samples were kept in a moisture-free, desiccated, environment prior to the start of the experiment.

Density

Density (ρ) of the polymers were measured with a density apparatus (Mettler ME-40290) and a precision balance, using methanol (MeOH). Small pieces (0.2–0.3 g) were cut from plaques and massed both above the methanol (m_1) and immersed (m_2) in it. Measurements were performed in triplicate and ρ values were calculated as

$$\rho = (m_1/m_2)\rho_{\mathrm{MeOH}}. \quad (11)$$

Thermal transitions and crystallinity

Glass transition temperatures (T_g), melting temperatures (T_m), and melting enthalpies (ΔH) were determined using a PerkinElmer DSC7 differential scanning calorimeter (DSC). Three pieces with masses of 4–7 mg were cut from the plaques and tested as molded by heating at a rate of 10°C/min. Analysis was performed using the resident software. T_g values were taken from the inflection point and T_m values from the peak. Crystalline weight fraction (x_c) of the polymers was calculated from eq. (2) using the following values for ΔH_c: 203 J/g for PA6, 207 J/g for PA66, and 210 J/g for PA46.[7] The standard deviations in the measurements were ±2°C for glass transition temperature (T_g) and melting temperature (T_m), ±4 J/g for melting enthalpy (ΔH), and ±0.04 for crystalline weight fraction (x_c).

Absorption

Absorption measurements were performed at room temperature [(25 ± 1)°C]. After the initial mass and dimensions were measured, the dry plaques were immersed in DI water. Periodically, the plaques were removed from the water, unabsorbed water was wiped from their surfaces with an absorbent, lint-free tissue, their mass, and dimensions were quickly measured, and then they were reimmersed. This process was repeated until mass and dimensions ceased to change. Mass was measured with an electronic balance (Toledo Mettler AG245) that had precision of ±0.1 mg. Dimensions were measured with a caliper (Mitutoyo Digimatic, CD-6'' BS). The precision of the caliper was ±0.01 mm. Error in m_f/m_o and L_f/L_o was computed using standard error propagation techniques. Error in D and α was estimated graphically and was $\sim$ 25%.

RESULTS AND DISCUSSION

Density

Table I shows the densities of the PA pellets and plaques. The densities of both the dry pellets and dry plaques (ρ_o) are in excellent agreement with the literature values for these materials.[11] Although these PAs can absorb more than 5% of their weight of water, the densities of moisture-saturated plaques (ρ_f) changed very little. Ratios of the initial-to-final density (ρ_o/ρ_f) showed differences of less than 1%. Somewhat surprisingly, densities increased very slightly, even though the density of water is less than that of the PAs. This behavior has been reported previously for PA610 and PA66.[3]

Thermal transitions and crystallinity

The thermal properties of polymer substrates, listed in Table II, were taken from the first heat to reflect the state of the material after molding. These were similar to values from the second heat and are in general agreement with the literature values.[7,11] The glass transition temperature of the PAs was $T_g \approx$ 35–40°C and probably can be attributed to motions associated with the amide group within the amorphous portions of the PAs. The melting temperatures of these polymers varied more widely. PA6 had the lowest T_m and PA46 the highest. Crystallinity ranged from 37% for injection-molded PA6 to 49% for PA46. The compression-molded PA66 and PA6 samples had about the same crystalline content of $\sim$ 40%.

TABLE II
Thermal Properties of the Various PA Plaques

Polymer	Molding	B_o (mm)	T_g (°C)	T_m (°C)	ΔH (J/g)	x_c
PA66	Compress	1.6	33	264	90	0.43
PA6	Compress	0.8	39	222	84	0.41
		1.6	41	222	85	0.42
		3.2	37	222	85	0.42
	Inject	1.6	40	221	74	0.37
		3.2	37	222	79	0.38
PA46	Compress	1.6	36	286	104	0.49

Absorption

Mass change

Figure 1 shows the increase in mass absorption ratio (m/m_o) with time (t) for 1.6-mm thick compression-molded PA6 plaques immersed in water at room temperature (25°C). During the early stages, plaques absorbed water rapidly and then slowed as they approached their saturation limit. These PA6 plaques reach their equilibrium of $m_f/m_o = 1.088$ (or 8.8% water uptake) after about 370 h of water immersion.

Diffusion coefficient

Values of D were determined from the early stages of absorption using eq. (3). Per eq. (3), a plot of Q versus t, where $Q = (\pi/16)B_o^2[(m - m_o)/(m_f - m_o)]^2$, give linear data, which passed through the origin. During the early stages of absorption, the slope was equal to D. An example is shown below in Figure 2 for 1.6-mm thick compression-molded PA6 plaques immersed in water at room temperature, where data from Figure 1 was replotted according to eq. (3). For these specimens, $D = 4.6 \times 10^{-9}$ cm^2/s. Error in the slope is $\sim$ 25%.

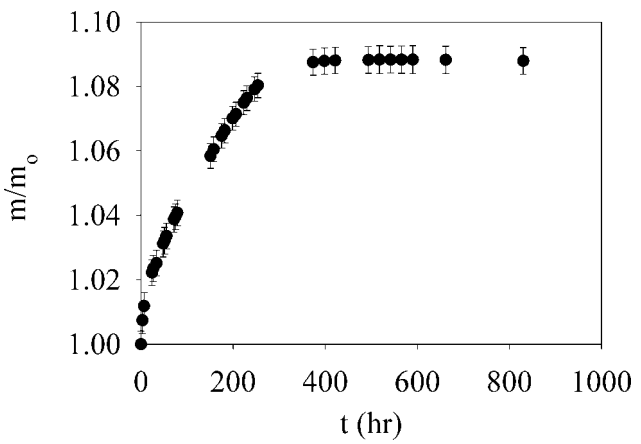

Figure 1 Mass absorption ratio (m/m_o) versus time (t) for 1.6-mm thick compression-molded PA6 plaques immersed in water at room temperature (25°C).

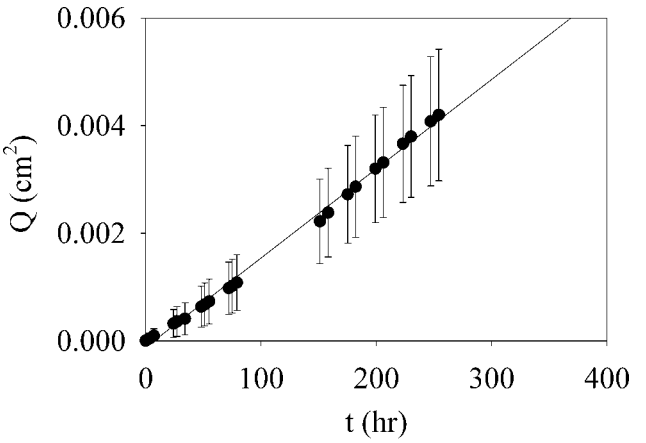

Figure 2 Early stages of absorption for 1.6-mm thick compression-molded PA6 plaques immersed in water at room temperature plotted according to eq. (3).

Once this value of the diffusion coefficient (D) has been determined, it can then be used to describe increases in mass and dimension. Figure 3 shows the mass absorption ratio (m/m_o) versus time (t) for the same 1.6 mm thick compression-molded PA6 plaques immersed in water at room temperature. The points are the experimental data and the solid line represents the full range of the calculated change in m/m_o using eqs. (4) and (5) with $D = 4.6 \times 10^{-9}$ cm^2/s and $m_f/m_o = 1.088$. Earlier investigators have suggested that the absorption of water by PAs can be approximated as Fickian.[5,14] Thus, agreement between experimental and calculated values was reasonably good during the early stage. However, it also has been demonstrated that D values increase as water concentration within PAs rises.[5,14] This explains the deviation from the calculated sorption curve shown in Figure 3. As sorption progressed,

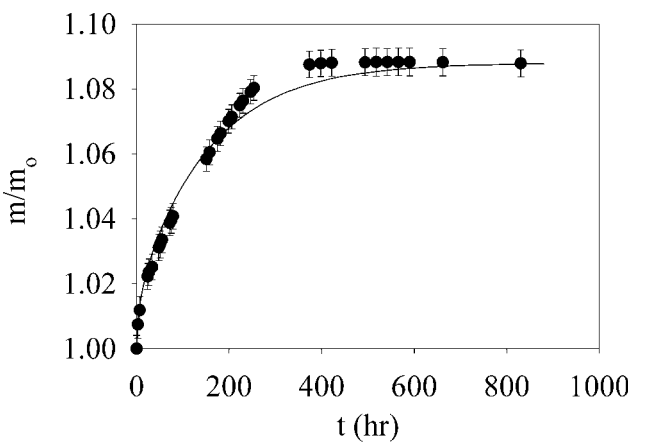

Figure 3 Experimental and calculated values for mass absorption ratio (m/m_o) versus time (t) for 1.6 mm thick compression-molded PA6 plaques immersed in water at room temperature.

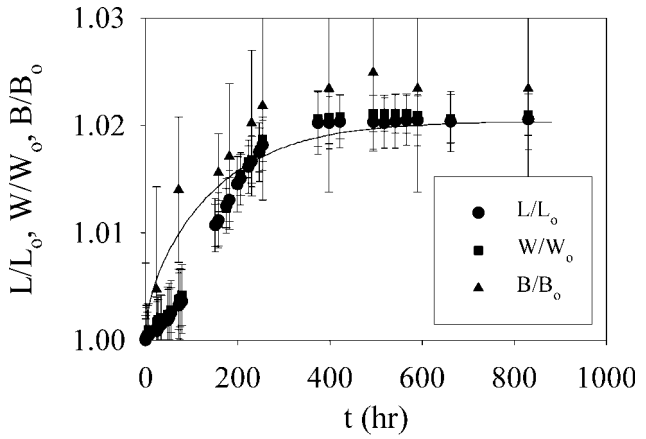

Figure 4 Length, width, and thickness ratios (L/L_o, W/W_o, and B/B_o) versus time (t) for 1.6 mm thick compression-molded PA6 plaques immersed in water at room temperature.

D increased. As a result, the calculated curve underestimated the latter stages of sorption.

Dimensional changes

Figure 4 shows the length, width, and thickness ratios (L/L_o, W/W_o, and B/B_o) versus time (t) for the same 1.6-mm thick compression-molded PA6 plaques immersed in water. The points are experimental data. The plaques expanded isotropically. Within experimental error, L/L_o, W/W_o, and B/B_o gave the same values. (As all other specimens also expanded isotropically, further discussion will be limited to the changes in length.) Dimensional changes lagged behind water absorption, as evident in the contrasting time-dependent curves. Swelling ceased at the same time as mass absorption, t_f = 370 h. The equilibrium length ratio (L_f/L_o) for these specimens was L_f/L_o = 1.020 (or 2.0% growth).

Although the sorption curve initially showed linear behavior before leveling off, the swelling curve was sigmoidal or S-shaped as noted by other investigators.[1,2,4–6] The solid line represents the changes calculated using eqs. (5) and (6) with $D = 4.6 \times 10^{-9}$ cm^2/s. Agreement between the experimental and calculated values is only fair. The calculation over-predicts the increase in dimensions in the early stages and under-predicts in the latter stages. The initial lag can be explained by a mechanical force imbalance between the swollen outer skin and the dry inner core of the specimens.[1,6,9,15] As the outer skin absorbs water, it swells. It cannot, however, do so freely. The stiffer, more abundant core tempers the initial expansion. As discussed earlier, the under-prediction in the latter stages is likely due to an increase in the diffusion coefficient as the plaques imbibe water. Although beyond the scope of this study, a swelling curve with a better fit could be calculated numerically using models that first account for the change in water concentration throughout the specimen and then balance the stresses associated with swelling.[1,5]

Effect of thickness

Figure 5 shows the mass absorption ratios (m/m_o) versus time (t) for compression-molded PA6 plaques of various thicknesses (B_o) immersed in water at room temperature. The points are experimental data. The thicker the plaque, the more slowly m/m_o values rose toward equilibrium. Equilibrium water absorption (m_f/m_o) for the three thicknesses ranged between 1.085 and 1.088 with an average value of $m_f/m_o = 1.086 \pm 0.010$ (or 8.6% water uptake). Values of t_f were estimated from graphs of m/m_o vs. t. For the thinnest plaques, t_f = 90 h; for the thickest, t_f = 1380 h. Although the saturation times varied widely, the equilibrium mass ratios (m/m_o), diffusion coefficients (D), and α values were independent of thickness. The solid lines in Figure 5 represent the calculated change in m/m_o [eqs. (4) and (5)]. Agreement at short times was good. (We calculated D values for each thickness. Because these values were approximately equal to each other, we used an overall average to calculate the curves shown in Fig. 5.)

Figure 6 shows the corresponding length absorption ratio (L/L_o) versus time (t) for compression-molded PA6 plaques of various thicknesses (B_o). The points are experimental data and the solid lines represent the L/L_o values calculated from eqs. (5) and (6) using an average D value computed from the PA6 specimens, $D = 4.6 \times 10^{-9}$ cm^2/s. The dimensional changes behaved similarly to the mass changes. The thinnest plaques grew the fastest, the thickest ones grew the slowest, yet all arrived at the same equilibrium length ratio, $L_f/L_o = 1.019 \pm 0.007$ (or 1.9% growth). Again, the time required for the plaques to reach L_f/L_o coincided with the time to reach m_f/m_o.

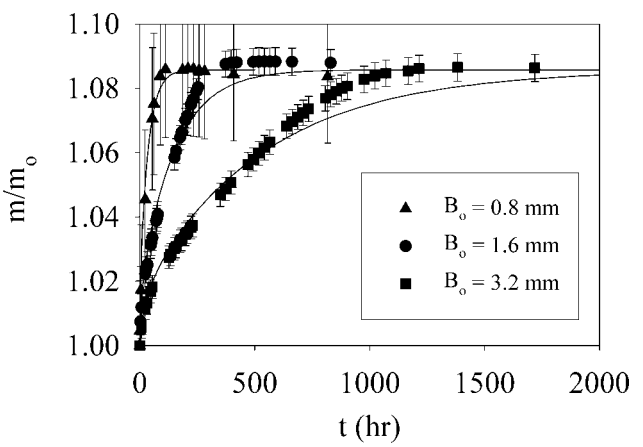

Figure 5 Mass absorption ratio (m/m_o) versus time (t) for compression-molded PA6 plaques of various thickness (B_o).

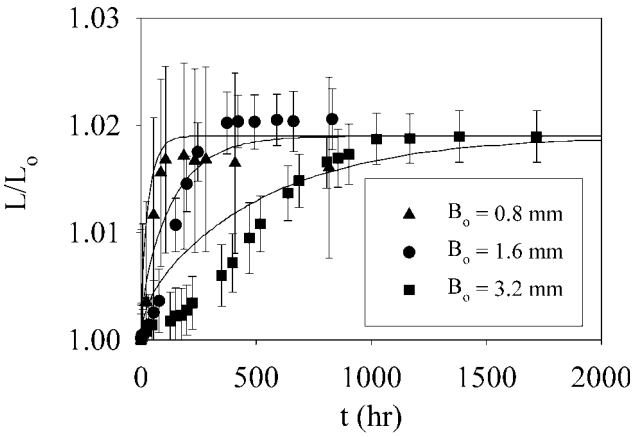

Figure 6 Length absorption ratio (L/L_o) versus time (t) for compression-molded PA6 plaques of various thickness (B_o) immersed in water at room temperature.

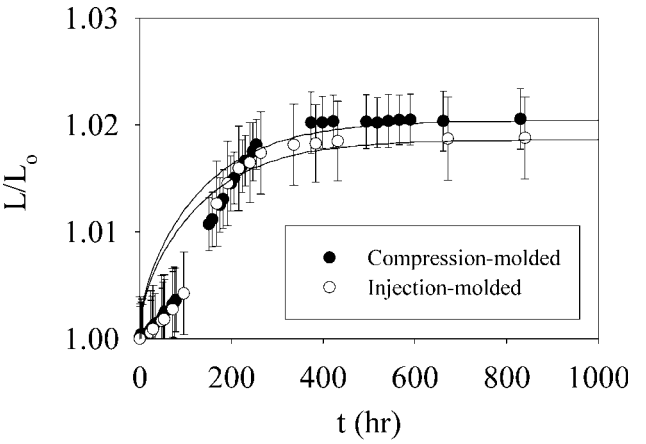

Figure 8 Length absorption ratio (L/L_o) versus time (t) for compression-molded and injection-molded PA6 plaques of the same thickness (B_o = 1.6 mm) immersed in water at room temperature.

Effect of processing

Figures 7 and 8 show a comparison of sorption behavior for compression-molded and injection-molded PA6 plaques with the same thickness, B_o = 1.6 mm. The points are experimental data, and the solid lines were calculated with $D = 4.6 \times 10^{-9}$ cm^2/s. The injection-molded plaques absorbed more water (10.4%) than their compression-molded counterparts (8.6%). The greater level of absorption of the injection-molded specimens was probably due to their lower crystallinity. Disparity in the thickness and aspect ratio of the compression-molded and injection-molded specimens also may have contributed to the observed differences in absorption. Even though m_f/m_o differed between the two molding methods, compression-molded and injection-molded PA6 plaques gave similar L_f/L_o, D, and α values.

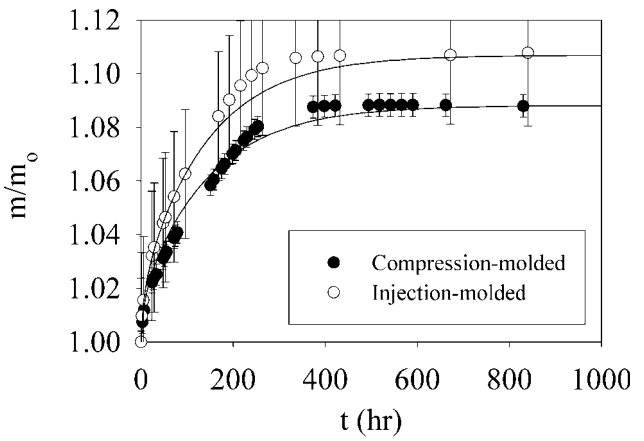

Figure 7 Mass absorption ratio (m/m_o) versus time (t) for compression-molded and injection-molded PA6 plaques of the same thickness (B_o = 1.6 mm) immersed in water at room temperature.

Effect of amide content

Amide fraction is largely responsible for distinguishing the properties of one type of PA from another (e.g., PA6 from PA46). As the amide content increases, so does the polarity and moisture absorption. Figures 9 and 10 show the absorption behavior of compression-molded plaques of the various PAs, all with the same thickness, B_o = 1.6 mm. The points are experimental data and the solid lines represent the calculated change of mass and dimensions with the progression of time. As expected, the most polar of the PAs, PA46, absorbed the most water and absorbed it the most quickly. PA6 and PA66 have identical amide content and similar crystallinity. Nevertheless, there were marked differences between their sorption behaviors. PA66 absorbed less water than PA6 and took much longer to reach equilibrium.

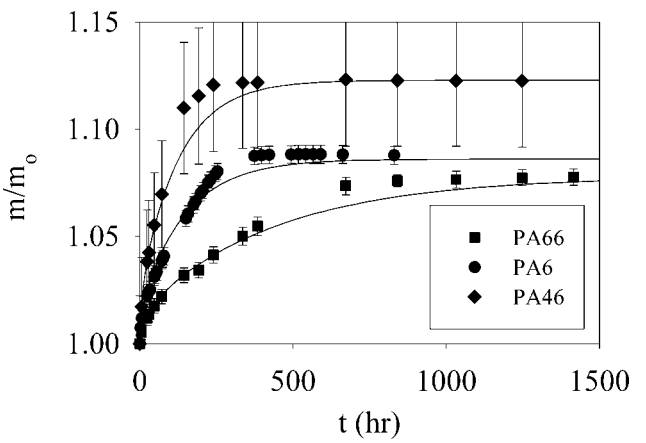

Figure 9 Mass absorption ratio (m/m_o) versus time (t) for compression-molded PA plaques of the same thickness (B_o = 1.6 mm) immersed in water at room temperature.

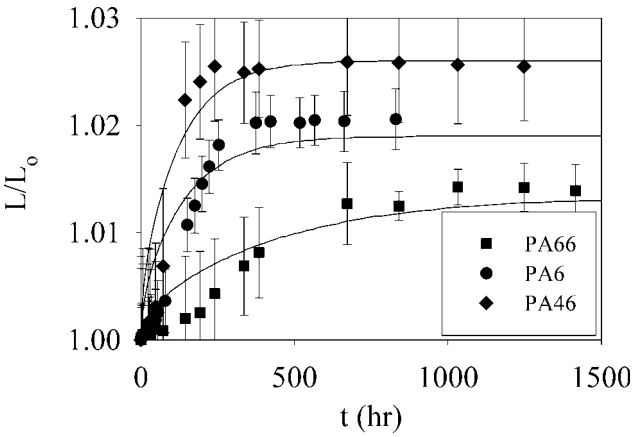

Figure 10 Length absorption ratio (L/L_o) versus time (t) for compression-molded PA plaques of the same thickness (B_o = 1.6 mm) immersed in water at room temperature.

Once more, agreement between experimental and calculated m_f/m_o values was reasonably good at early times but as the sorption progressed, the calculated values lagged behind the experimental ones presumably due to an increase in diffusivity as the concentration of water rose throughout the material. The time-dependent swelling data for all three polymers was sigmoidally shaped, initially lagging behind absorption. As previously described, in the early stages, expansion of the swollen outer skin is impeded by tension in the stiffer, dryer inner core. Equilibrium absorption times (t_f) were estimated from graphs of m/m_o vs. t. Values of t_f were as follows: t_f = 1420 h for PA66, t_f = 370 h for PA6, and t_f = 330 h for PA46. In general, similar values of t_f could be estimated using eqs. (4) and (5) with $(m - m_o)/(m_f - m_o) = 0.95$. Table III summarizes values of m_f/m_o, L_f/L_o, D, and α of the various PAs. These values generally agreed with those reported in the literature.[5–7,14,16–18]

Table IV shows a comparison of the equilibrium length ratios (L_f/L_o) that were either directly measured or estimated using eqs. (7) and (8). Since the density of the saturated PAs differed very little from their dry counterparts, eqs. (7) and (8) gave nearly identical results. However, both equations overestimated L_f/L_o values by 50–100%. This overestimation probably arose due to water plasticizing the PAs and subsequently relieving not only the stresses of the swollen skin,[1] but also the residual stresses that are present throughout all molded thermoplastics.[15] At a molecular level, the relaxation equates to elongated polymer chains slipping pass each other to relieve the swelling stresses that otherwise would have driven expansion.

Although the simplicity of this estimate is clearly deficient from a scientific perspective, it has value for engineering estimates. Dimensional changes due to liquid absorption are relatively easy to measure for highly absorbent systems such as water and these three PAs. However, direct measurement on other engineering thermoplastics is more tedious. Most engineering thermoplastics are hygroscopic, but absorb much less water than PAs—their equilibrium moisture content after long immersion times in water usually is ≤0.5%. Moreover, measurement of small length changes is generally more difficult and less precise than the measurement of mass. Thus, where moisture absorption is low and the specific gravity of the polymer is near one, values of L_f/L_o with a generous safety margin can be estimated directly from the equilibrium mass absorption ratios (m_f/m_o) using eq. (8). On the basis of our experiences with other engineering polymers that absorb smaller amounts of water than PAs, we believe that the same general approach could be used for estimating their dimensional changes from sorption data.

CONCLUSIONS

With the greatest polarity, PA46 absorbed more water than less-polar PAs and, therefore, was more susceptible to moisture-induced dimensional growth. Thick samples took longer to reach saturation, but D values were independent of thickness for a given polymer. Changes in the dimensions coincided with changes in mass. Swelling and sorption followed different paths, but arrived at their respective equilibrium values at the same time. Within experimental error, dimensional expansion due to water absorption was isotropic, i.e., expansion was the same in all directions. Injection-molded samples absorbed slightly more water than compression-molded ones, but absorption rates were the same (same D and α values). For a given polymer, equilibrium moisture absorption and diffusion coefficients derived from a single experiment of this type can be used to estimate dimensions of swollen parts and equilibrium

TABLE III
Absorption Parameters for the Various Compression-Molded PA Plaques with B_o = 1.6 mm

Polymer	x_a	x_c	m_f/m_o	L_f/L_o	D (cm^2/s)	α (s/cm^2)
PA66	0.167	0.43	1.078 ± 0.004	1.013 ± 0.003	$(1.7 \pm 0.4) \times 10^{-9}$	$(1.9 \pm 0.5) \times 10^{8}$
PA6	0.167	0.41	1.088 ± 0.004	1.020 ± 0.006	$(4.6 \pm 1.1) \times 10^{-9}$	$(5.0 \pm 1.4) \times 10^{7}$
PA46	0.200	0.49	1.123 ± 0.031	1.026 ± 0.005	$(6.2 \pm 1.4) \times 10^{-9}$	$(4.3 \pm 1.1) \times 10^{7}$

TABLE IV
Measured and Calculated Equilibrium Length Ratios (L_f/L_o) of the PA Plaques

Polymer	Molding	B_o (mm)	m_f/m_o Measured	L_f/L_o Measured	L_f/L_o Equation (7)	L_f/L_o Equation (8)
PA66	Compress	1.6	1.078 ± 0.004	1.013 ± 0.003	1.024 ± 0.002	1.025 ± 0.001
PA6	Compress	0.8	1.086 ± 0.021	1.017 ± 0.009		1.028 ± 0.006
		1.6	1.088 ± 0.004	1.020 ± 0.006	1.026 ± 0.005	1.028 ± 0.001
		3.2	1.085 ± 0.004	1.019 ± 0.006		1.028 ± 0.001
	Inject	1.6	1.107 ± 0.026	1.019 ± 0.004		1.034 ± 0.008
		3.2	1.101 ± 0.005	1.015 ± 0.001		1.033 ± 0.002
PA46	Compress	1.6	1.123 ± 0.031	1.026 ± 0.005	1.038 ± 0.010	1.026 ± 0.005

swelling times, independent of sample thickness, processing, and modest variations in crystallinity.

We thank Entegris management for supporting this work and allowing publication. Also thanks to DSM Engineering Plastics for providing the injection-molded PA6 plaques as well as S. I. Moon for his suggestions on the technical content and text.

APPENDIX

Estimating dimensional changes with the diffusion coefficient

A formal derivation of eq. (6) is given below. Consider a thin sheet immersed in liquid. The change in mass (m) with time (t) is described by the following expression[9]

$$(m - m_o)/(m_f - m_o) = S, \tag{12}$$

where m_o is the initial mass of the dry sheet, m_f is the equilibrium mass of the liquid-saturated sheet, and S is an infinite series,

$$S = 1 - \sum_{n=0}^{\infty} \{8/\pi^2(2n+1)^2 \exp[-D(2n+1)^2\pi^2 t/B_o^2]\} \tag{5}$$

that contains the diffusion coefficient (D) and initial sample thickness (B_o). Equation (5) assumes that at $t = 0$, $m = m_o$.

The masses of eq. (12) can be written in terms of densities (ρ, ρ_o, and ρ_f) and volumes (V, V_o, and V_f),

$$m = \rho V, \tag{13}$$

$$m_o = \rho_o V_o, \tag{14}$$

and

$$m_f = \rho_f V_f, \tag{15}$$

where ρ and V represent the time-dependent values, ρ_o and V_o are the initial values, and ρ_f and V_f are equilibrium values. Combining eqs. (12)–(15) give

$$(\rho V - \rho_o V_o)/(\rho_f V_f - \rho_o V_o) = S. \tag{16}$$

If the density of the liquid and the sheet do not differ greatly and absorption is amount of liquid absorbed is small, then

$$\rho \approx \rho_o \approx \rho_f \tag{17}$$

and equation can be rewritten as

$$(V - V_o)/(V_f - V_o) = (V/V_o - 1)/(V_f/V_o - 1) = S. \tag{18}$$

The volumes of the thin sheets can be described in terms of their lengths (L, L_o, L_f), widths (W, W_o, W_f), and thicknesses (B, B_o, B_f),

$$V = LWB, \tag{19}$$

$$V_o = L_o W_o B_o, \tag{20}$$

and

$$V_f = L_f W_f B_f. \tag{21}$$

Combining eqs. (18)–(22) and rearranging give,

$$[(L/L_o)(W/W_o)(B/B_o) - 1]/[(L_f/L_o)(W_f/W_o)(B_f/B_o) - 1] = S. \tag{22}$$

If the sheet expands isotropically during absorption, then

$$L/L_o = W/W_o = B/B_o, \tag{23}$$

$$L_f/L_o = W_f/W_o = B_f/B_o, \tag{24}$$

and eq. 22 can be rewritten as

$$[(L/L_o)^3 - 1]/[(L_f/L_o)^3 - 1] = (L^3 - L_o^3)/(L_f^3/L_o^3) = S. \tag{25}$$

Now let

$$L = L_o + \Delta L \tag{26}$$

and

$$L_f = L_o + \Delta L_f. \quad (27)$$

By combining eqs. (25)–(27) and expanding the numerator and denominator, one obtains the following expression

$$(\Delta L^3 + 3\Delta L^2 L_o + 3\Delta L L_o^2)/(\Delta L_f^3 + 3\Delta L_f^2 L_o + 3\Delta L_f L_o^2) = S. \quad (28)$$

Because $L \gg \Delta L$ or ΔL_f, then

$$3\Delta L L_o^2 \gg 3\Delta L^2 L_o \gg \Delta L^3, \quad (29)$$

$$3\Delta L_f {L_o}^2 \gg 3\Delta {L_f}^2 L_o \gg \Delta {L_f}^3, \quad (30)$$

and eq. (28) reduces to

$$\Delta L/\Delta L_f = (L - L_o)/(L_f - L_o) = S \quad (31)$$

or

$$L/L_o = 1 + S[(L_f/L_o) - 1] \quad (6)$$

Similar equations can be derived for width and thickness,

$$W/W_o = 1 + S[(W_f/W_o) - 1] \quad (32)$$

and

$$B/B_o = 1 + S[(B_f/B_o) - 1]. \quad (33)$$

Equations (6), (32), and (33) ignore the retardation of specimen swelling due to the competition between the expansion of the swollen skin and the tension in its core as well as any relaxation that occurs during sorption.

Estimating equilibrium dimensional changes from equilibrium mass

Measuring changes in mass is much easier and more precise than measuring the associated dimensional changes, especially for specimens where absorption is minimal. Therefore, it would be faster, easier, and likely more accurate to estimate L_f/L_o values (or W_f/W_o or B_f/B_o) from equilibrium-to-initial mass (m_f/m_o) ratio. This ratio can be written in terms of densities and volumes,

$$m_f/m_o = \rho_f V_f/\rho_o V_o. \quad (34)$$

As before, if dimensional changes are isotropic, then combining eqs. (20), (21), (24), and (34), and rearranging gives,

$$L_f/L_o = W_f/W_o = B_f/B_o = [(\rho_o/\rho_f)(m_f/m_o)]^{1/3}. \quad (7)$$

If the density of the material does not change appreciably during absorption ($\rho_o \approx \rho_f$), then eq. (7) reduces to

$$L_f/L_o = W_f/W_o = B_f/B_o = (m_f/m_o)^{1/3}. \quad (8)$$

References

1. Crank, J. A. J Polym Sci 1953, 11, 151.
2. Boasson, E. H.; Scheers, H. J. H. J Polym Sci 1955, 17, 311.
3. Starkweather, H. W., Jr. J Appl Polym Sci 1959, 2, 129.
4. Takagi, Y.; Hattori, H. J Appl Polym Sci 1965, 9, 2177.
5. Inoue, K.; Hoshino, S. J Polym Sci Part B: Polym Phys 1976, 14, 1513.
6. Hunt, D. G.; Darlington, M. W. Polymer 1980, 21, 502.
7. Brandrup, J.; Immergut, E. H.; Grulke, E. A. Polymer Handbook, 4th ed.; Wiley: New York, 1999.
8. Runt, J. P. In Encyclopedia of Polymer Science and Engineering, 2nd ed.; Mark, H. F.; Kroschwitz, J. I., Eds.; Wiley: New York, 1986; Vol. 4.
9. Crank, J. The Mathematics of Diffusion; Oxford University Press: London, 1970.
10. Saechtling, H. International Plastics Handbook, 2nd ed.; Oxford University Press: New York, 1987.
11. Osswald, T. A.; Menges, G. Materials Science of Polymers for Engineers; Hanser: New York, 1995.
12. Brydson, J. A. Plastics Materials, 6th ed.; Butterworth-Heinemann: Boston, 1995.
13. Weast, R. C. Handbook of Chemistry and Physics, 73rd ed.; CRC Press: Boca Raton, FL, 1992.
14. Asada, T.; Onogi, S. J Colloid Sci 1963, 18, 784.
15. Paterson, M. W. A.; White, J. R. Polym Sci Eng 1993, 33, 1475.
16. Jang, S. P.; Kim, D. Polym Eng Sci 2000, 40, 1635.
17. Lim, L.-T.; Britt, I. J.; Tung, M. A. J Appl Polym Sci 1999, 71, 197.
18. Adriaensens, P.; Pollaris, A.; Rulkens, R.; Litvinov, V. M.; Gelan, J. Polymer 2004, 45, 2465.
19. Kishimoto, A.; Fujita, H. J Polym Sci 1958, 28, 569.